

Langmuir-probe measurements in flowing-afterglow plasmas

R. Johnsen, E. V. Shun'ko, and T. Gougousi

Department of Physics and Astronomy, University of Pittsburgh, Pittsburgh, Pennsylvania 15260

M. F. Golde

Department of Chemistry, University of Pittsburgh, Pittsburgh, Pennsylvania 15260

(Received 18 July 1994)

The validity of the orbital-motion theory for cylindrical Langmuir probes immersed in flowing-afterglow plasmas is investigated experimentally. It is found that the probe currents scale linearly with probe area only for electron-collecting but not for ion-collecting probes. In general, no agreement is found between the ion and electron densities derived from the probe currents. Measurements in recombining plasmas support the conclusion that only the *electron* densities derived from probe measurements can be trusted to be of acceptable accuracy. This paper also includes a brief derivation of the orbital-motion theory, a discussion of perturbations of the plasma by the probe current, and the interpretation of plasma velocities obtained from probe measurements.

PACS number(s): 52.25.-b, 52.70.Ds, 52.30.-q

I. INTRODUCTION

Largely as a result of the work of Smith *et al.* [1], the use of cylindrical Langmuir probes to measure absolute electron and ion densities in flowing-afterglow plasmas has become rather common in recent years. The “orbital-limited” or “orbital-motion” theory of probes that is usually used in the analysis of probe data has the virtue of simplicity and there is good, although indirect experimental evidence that accurate electron-density measurements can be made if the probes are used “properly.” What constitutes proper use, however, is not entirely clear. The problem is of considerable interest in the case of measurements of electron-ion and ion-ion recombination rates since the results depend directly on the absolute values of the electron or ion densities.

In principle, *ion-collecting* probes should produce far smaller perturbations since the probe currents are smaller by the square root of the electron to ion mass ratio. It appeared to us that ion-collecting probes might be preferable for our studies of electron-ion recombination processes, especially since some authors [2] had used ion-collecting probes in flowing-afterglow measurements of ion-ion recombination rates. Our experiments with ion-collecting probes, however, gave results that were inconsistent with those obtained from electron-collecting probes and we were initially unable to decide which of two determinations could be trusted. Recent Langmuir-probe measurements in discharge plasmas by Sudit and Woods [3] pointed out a possible source of the problem. Their results indicated that the orbital-motion theory overestimates ion densities by factors of up to 10 under their experimental conditions and the authors suggested that the neglect of ion-neutral-species collisions in the orbital-motion theory may be the principal cause of the discrepancy. A discharge plasma, however, differs considerably from an afterglow plasma and those findings may have no direct bearing on the use of probes in an

afterglow plasma. While the literature on Langmuir probes is very extensive, and several attempts have been made to incorporate collisions into the theory (see, e.g., the review by Chung, Talbot, and Touryan [4], and references cited therein), a rigorous theory of probes in the presence of collisions does not seem to exist. In their review, Chung, Talbot, and Touryan state that the numerical work required to make practical use of some of the more rigorous theories is prohibitive, which would make them unattractive to most experimentalists.

The problems that we encountered motivated us to perform a series of test measurements and to examine in some detail the use of probes in flowing-afterglow plasmas. Our main interest was to test the orbital-motion theory by checking some of its predictions, such as scaling of the probe currents with surface area and the consistency of ion- and electron-density measurements. Measurements of electron-ion recombination rates are the principal motivation for this work, but we will describe such measurements here only to the extent that they support the validity of the orbital motion theory of electron-collecting Langmuir probes.

A brief rederivation of the probe theory in the orbital-limited regime is given to show which assumptions are made and where they are likely to fail. Electrical perturbations of the plasma by the probes are discussed in some detail. The dynamics of flowing-afterglow plasmas is not the subject of the paper, but we include some remarks on Langmuir-probe measurements of plasma velocities in order to point out some inconsistencies in their interpretation.

II. THEORETICAL CONSIDERATIONS

A. The “orbital-limited” theory of Langmuir probes for cylindrical probes

The calculation of the charged-particle current to an attracting cylindrical probe is a simple matter of classical

mechanics, provided that the range of the shielded probe potential $V(r)$ is large compared to the radius of the probe r_p and that the particles do not suffer collisions while being accelerated to the probe. The derivation given here is essentially the same as that given by Mott-Smith and Langmuir [5] but it is expressed in terms that make the analogy with atomic collision physics more apparent. As is customary, we assume that the length of probe is far larger than its diameter. The range of the probe potential is approximately given by the sheath radius given by Bettinger and Walker [6],

$$R_S = 1.66\lambda_D(eV/kT)^{3/4} + r_p, \quad (1)$$

where

$$\lambda_D = (\epsilon_0 kT/n_e e^2)^{1/2} \quad (2)$$

is the Debye shielding length, ϵ_0 is the permittivity of the vacuum, k is Boltzmann's constant, T is the electron temperature, n_e is the electron density, and e is the electronic charge. One considers the motion of a charged particle of mass m with initial velocity $v_0 = (v_t^2 + v_r^2)^{1/2}$ and impact parameter h , where the subscripts designate the tangential and radial components of the velocity, motion parallel to the probe being irrelevant. If the effective potential energy $U(r)$ (sum of electrostatic and centrifugal potential energies)

$$U_{\text{eff}}(r) = eV(r) + \frac{1}{2}mv_0^2(h/r)^2 \quad (3)$$

has no centrifugal barriers, i.e., $V(r)$ approaches zero more slowly than the $1/r^2$ centrifugal potential, the particle will approach the probe axis to a closest distance r_c at which the radial part of its kinetic energy becomes zero, i.e.,

$$U_{\text{eff}}(r_c) = mv_0^2/2. \quad (4)$$

For some initial conditions, r_c will be less than the probe radius r_p and the particle will strike the probe. For a given probe potential $V(r_p)$ and initial kinetic energy $mv_0^2/2$, the largest impact parameter for which a particle strikes the probe is given by

$$h_{\text{max}} = r_p [1 - eV(r_p)/(mv_0^2/2)]^{1/2} \quad (5)$$

and the probe has a collision cross section (effective target area) of

$$\begin{aligned} Q &= 2Lh_{\text{max}} \\ &= 2Lr_p [1 - eV(r_p)/(mv_0^2/2)]^{1/2}. \end{aligned} \quad (6)$$

The electrical current to the probe is then obtained by multiplying Q with the flux of particles having velocities around v_0 and integrating over velocity,

$$I = 2Lne \int_0^\infty r_p [1 - eV(r_p)/(mv_0^2/2)]^{1/2} S v_0 f(v_0) dv_0, \quad (7)$$

where $f(v_0)$ is the distribution function of velocities in the plane of motion. The range of integration should be restricted to values of v_0 and $V(r_p)$ for which the root in the integrand is real. Rather than incorporating this con-

dition into the integration limits, we have multiplied the integrand with a function S which is defined to be zero for $[1 - eV(r_p)/(mv_0^2/2)] < 0$ but equal to unity elsewhere.

The case of greatest interest in afterglow plasmas is that where the initial velocities v_0 have a Maxwellian distribution in the plane of motion,

$$f(v_0) = (m/kT)v_0 \exp(-mv_0^2/2kT). \quad (8)$$

It is convenient to make the substitutions

$$y = V(r_p)e/kT \quad \text{and} \quad x = v_0(m/2kT)^{1/2}. \quad (9)$$

The probe current then becomes

$$\begin{aligned} I &= 2n_e e (A_p/\pi)(2kT/m)^{1/2} \\ &\quad \times \int_0^\infty (1 - y/x^2)^{1/2} S x^2 \exp(-x^2) dx, \end{aligned} \quad (10)$$

where $A_p = 2\pi r_p L$ is the surface area of the probe.

The integral approaches the value $y^{1/2}/2$ in the limit $-y/x^2 \gg 1$, which corresponds to the important case of a strongly attracting potential. The probe current then is

$$I = 2n_e e (A_p/\pi)(2kT/m)^{1/2} (eV_p/kT)^{1/2}. \quad (11)$$

The current is quite large; for typical probe dimensions ($2r_p = 25 \mu\text{m}$, $L = 0.5 \text{ cm}$), an electron-collecting probe draws a current of $I = 107 \mu\text{A}$ at $V_p = 1 \text{ V}$. Equation (11) is identical to that derived by Mott-Smith and Langmuir [5] and it is commonly used to deduce electron and ion densities from measured probe currents. The integral in Eq. (10) can be expressed in terms of error functions, but the resulting expressions are awkward. A numerical integration shows that the approximate form in Eq. (11) is excellent for $eV_p/kT > 1$. In practice, the probe potential V_p is measured with respect to a reference electrode (often the walls of the plasma chamber) rather than the potential of the plasma and n_e is obtained from the slope of a graph of I^2 vs V_p . The assumption is made that the potential drop between the plasma and the reference electrode is not affected by applying a bias voltage to the probe.

When the probe is operated at $V_p = 0$, Eq. (11) is not applicable. Instead, by integrating Eq. (10) one obtains the well-known formula for the current at space potential,

$$I = (n_e e A_p / 4)(8kT/\pi M)^{1/2}. \quad (12)$$

In a real plasma, both ions and electrons will contribute to the probe current. The total current then is the sum of the individual currents which can be calculated separately from Eq. (10), but in practice a positive probe bias potential reduces the current due to positive ions to completely negligible values and Eq. (11) is entirely satisfactory for an electron-collecting probe. At slightly negative bias voltages, both positive ions and electrons contribute to the current. In that case, a numerical integration of Eq. (10) for the charged particles of interest and summing the currents may be required for comparison with measured I - V curves.

The assumption that the effective potential contains no

centrifugal barrier is not critical in the range of electron densities of interest in afterglows (10^9 to 10^{11} cm^{-3}) since the sheath radius tends to be large compared to the diameter of the probe. If, for the purpose of estimation, we assume that the potential goes to zero at the sheath radius and remains zero outside of that radius, then a centrifugal barrier of height $\frac{1}{2}mv_0^2(h/R_s)^2$ is located at the sheath radius R_s . For impact parameters h greater than R_s the barrier exceeds the kinetic energy of the incoming particle so that the particle is reflected. This means that the impact parameters given by Eq. (5) should be restricted to values less than R_s , since particles with $h > R_s$ never come under the influence of the attracting potential and thus cannot be collected. The sheath radius R_s , however, depends on the probe voltage [see Eq. (1)] and it is not immediately obvious what fraction of ions will be reflected. To gain some insight into the magnitude of the effect, the impact parameters in a numerical integration of Eq. (10) were limited to values of less than the sheath radius given by Eq. (1). The results showed that for values of the ratio $\lambda_D/r_p > 1$ Eq. (10) still is an excellent approximation. If one reduces that ratio to less than 0.25, the current is reduced by about 25% below that given by Eq. (10). For a probe radius $r_p = 1.25 \times 10^{-3}$ cm (diameter of 25 μm) this will occur for $n_e > 10^{11}$ cm^{-3} . Thus there is no serious problem for electron densities below 10^{11} cm^{-3} .

Collisions between charged particles and neutral atoms are neglected in the orbital-limited theory. This appears to be justified if the mean free paths of the charged particles are very large compared to the sheath radius, but first of all this is not always true under experimental conditions. Table I lists typical values of relevant length scales. The mean free paths were estimated from momentum transfer cross sections obtained from mobility data. As may be seen, the electron mean free path is only about four times larger than the sheath radius at a typical probe voltage of 0.5 V and at an electron density of 10^{10} cm^{-3} .

The ion mean free path under the same conditions is actually smaller than the sheath radius. Furthermore, consideration of the mean free path for momentum transfer does not provide a satisfactory criterion since it does not take into account the fact that the fractional energy loss in an ion-atom collision,

$$\Delta E/E = 2m_i m_{\text{gas}} / (m_i + m_{\text{gas}})^2 \quad (13)$$

$$(\text{=0.165 for ions of mass 40 amu in helium}),$$

(assuming isotropic scattering) is several orders of magnitude larger than that in an electron-atom collision, in which case, since $m_e \ll m_{\text{gas}}$,

$$\Delta E/E \approx 2m_e/m_{\text{gas}} \quad (14)$$

$$(\text{= } 2.72 \times 10^{-4} \text{ for electrons colliding}$$

with helium atoms).

A single ion-atom collision, for instance of an ion that has been accelerated by the probe potential to energy of $E = 20kT$, may leave it with insufficient total energy ($-3.3kT$ on average for ions of mass 40 in helium) to escape from the potential well surrounding the probe. It will be collected by the probe with high probability. If the number of ion-atom collisions is small (low-pressure limit), collisions will enhance the current to the probe to values above that given by the orbiting theory. In the opposite case of a very large number of collisions, the ion current to the probe will be limited by diffusion and drift to the probe. The current then should decline with increasing pressures. The basic mechanisms are analogous to those considered in the theory of ion-ion recombination where one distinguishes a low-pressure (Thomson) regime and a high-pressure (Langevin) regime. Similar considerations led Schulz and Brown [7] to propose different models of ion-collecting probes, depending on the number of ion-neutral-species collisions in the sheath.

TABLE I. Typical values of the Debye lengths, sheath radii, ion and electron mean free paths, and Langmuir-probe radii.

Debye length	$\lambda_D = 3.77 \times 10^{-4}$ cm at $n_e = 10^{11}$ cm^{-3} ($T_e = 300$ K)
	= 1.12×10^{-3} cm at $n_e = 10^{10}$ cm^{-3}
	= 3.22×10^{-3} cm at $n_e = 10^9$ cm^{-3}
Sheath radius	$R_s = 5.9 \times 10^{-3}$ cm at $n_e = 10^{11}$ cm^{-3} and $V_p = 0.5$ V
	= 1.76×10^{-2} cm at $n_e = 10^{10}$ cm^{-3} and $V_p = 0.5$ V
	= 5.92×10^{-2} cm at $n_e = 10^9$ cm^{-3} and $V_p = 0.5$ V
Ion mean free path	$L_i = 0.8 \times 10^{-2}$ cm (Ar ⁺ ions in 1 Torr of He, at 300 K)
Electron mean free path	$L_e = 6.2 \times 10^{-2}$ cm (in 1 Torr of He, at 0.5 eV)
Probes	$R_p = 1.25 \times 10^{-3}$ cm ("large" probe)
	$R_p = 5 \times 10^{-4}$ cm ("small" probe)
	$L_p = 0.4\text{--}0.45$ cm

The situation is different in the case of electrons which have to suffer several hundred collisions before their total energy is rendered negative by an amount of the order of a few kT . Collisional "trapping" of an electron in the probe potential is thus unlikely. Again, an analogy can be made to theory of collision-stabilized recombination in an ambient gas. As is well known [8], collisional stabilization is far less efficient in electron-ion recombination in an ambient gas than in the case of ion-ion recombination.

These estimates suggest that the orbital-motion theory may be adequate for electrons but that it is likely to fail in the case of ions. A rigorous theory of ion collection in the presence of collisions is difficult to construct and there does not appear to be any theory that accomplishes this task. The experiments that will be described in the next section show that the orbital-motion theory fails severely in the case of ions. It appears unlikely that the theory can be "salvaged" by introducing minor corrections for collisional effects.

The derivation of the orbital-motion theory was made for a stationary (nonflowing) plasma, but there is no reason to believe [4] that a probe in the orbiting mode would behave differently in a flowing plasma since the random particle velocities [entering through Eq. (8)] are far larger than the subsonic flow velocities that are used in most experiments. The situation is not quite clear in the case of ions where the orbital-motion theory may not be applicable. For instance, if the ion current is limited by drift motion to the probe, the relevant drift velocities may not be large compared to the flow velocities. This introduces a further complication in the theory of ion collection, as was also pointed out by Chung, Talbot, and Touryan [4].

B. Perturbations of a flowing-afterglow plasma by Langmuir probes

Ideally, the presence of the probe should not affect any plasma parameters, such as densities, electric fields, or the electron temperature. Perturbations of a small region around the probe will have to be accepted as unavoidable, but the probe should not significantly perturb the quantity that one wishes to measure, for instance, the densities of electrons or ions.

Mechanical perturbations of the flowing plasma are not very important. The probe itself and its support structure obviously cause minor hydrodynamic perturbations of the plasma flow, but the effect will be limited to a small region downstream from the probe. In many flow tube experiments, far larger objects (e.g., gas inlets) are inserted without detrimental effects.

A potentially more severe perturbation of the plasma results from the fairly large electron currents that are drawn by a positively biased probe. A simple estimate shows that the current, even for small bias voltages, can easily exceed the "natural" or "flow" current of electrons that flows through a cross section of a flow tube,

$$I_{\text{flow}} = e \int_0^R n_e(z_p, r) v_{\text{flow}}(r) 2\pi r dr . \quad (15)$$

Here, z_p denotes the position of the probe in the flow tube and R is the tube radius. A numerical integration, using

a parabolic velocity profile and the electron density distribution obtained by solving the radial diffusion equation, gives the approximate formula

$$I_{\text{flow}} \approx 0.3e\pi R^2 n_e(r=0) v_{\text{flow}}(r=0) . \quad (16)$$

This current is approximately $25 \mu\text{A}$ at $n_e(r=0) = 10^{10} \text{ cm}^{-3}$ for a tube of radius $R = 2 \text{ cm}$ and central flow velocity $v_{\text{flow}}(r=0) = 5000 \text{ cm/s}$. The Langmuir-probe current at $n_e(r=0) = 10^{10} \text{ cm}^{-3}$ for a probe of diameter $2r_p = 25 \mu\text{m}$ and length 4 mm at a bias voltage of $+1 \text{ V}$, however, is close to $100 \mu\text{A}$, four times larger than the natural flow of electrons. The comparison is more favorable in a tube of larger cross section and higher flow velocity, but in most commonly used tubes the probe current would still be a significant fraction of the flow current.

The estimate shows that the probe has to attract electrons from the upstream region of the flow tube by producing an electric field that penetrates into that part of the tube. Thus a perturbation of the electron currents in the plasma will be present. However, a depletion of electrons, i.e., a reduction of the electron density, need not occur if this electric field reduces the diffusive current of electrons to the wall by an amount that is equal to the probe current. The probe then simply diverts part of the wall current and returns it to the walls indirectly through its circuitry. The maximum current that can be drawn is then limited only by the total electron current that enters the tube. One might also consider a mechanism in which the electric field penetrates into the plasma source (usually an electrical discharge) and draws additional electrons from the discharge plasma. This seems less likely, though, since in most such sources the electrons are produced indirectly by Penning ionization of atoms by metastable helium atoms and the electric field would not have much effect on the flux of metastable atoms from the source. Figure 1 schematically depicts the currents in a flow tube with electrically conducting walls. The direction of the arrows is chosen to conform to the convention for electrical currents, i.e., the electron current entering the flow tube is negative. It should not be assumed that

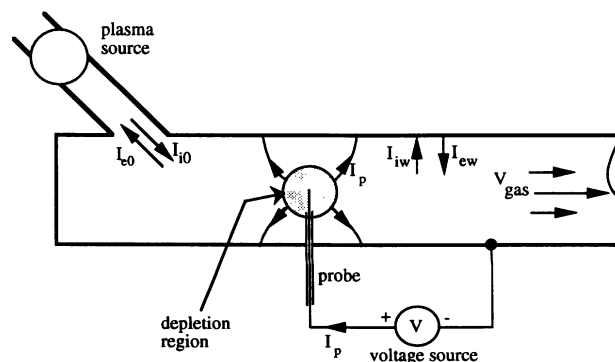


FIG. 1. Schematic diagram of electron and ion currents entering the flow tube from the discharge and leaving to either the probe or the flow tube wall.

the sum of the electron and ion currents entering the tube, $I_{e0} + I_{i0}$, is necessarily equal to zero since currents can also flow in the conducting walls. For the same reason, it is not necessary that the currents to the wall, I_{ew} and I_{iw} , add up to zero.

Under most conditions of interest, this mechanism of supplying electrons to the probe by reducing the wall current seems to work well and then there is no serious depletion of electrons over a significant range of bias voltages. The probe current rises with increasing bias voltages, as given by Eq. (11), until it saturates at some value which may approach the total current entering the tube. The magnitude of the electric drift field that is needed to supply the probe current I_p is quite small. It is approximately given by

$$E_d = (I_p) / (An_e e \mu), \quad (17)$$

where μ is the electron mobility ($\approx 760 \times 10^4$ cm²/V s for helium at 1 Torr [9] and A is a characteristic cross section of the current path. Using the same numbers as in Eq. (16), one obtains values of $E \approx 0.5 \times 10^{-3}$ V/cm if the current flows through the tube cross section $A = \pi R^2$. A field of this magnitude can be produced by a negligible depletion of less than 10^4 electrons in a sphere of 1 cm radius around the probe (see Fig. 1). The field is small compared to the radial ambipolar space charge field which confines the electrons and which controls the radial outflow of ions. The ambipolar space charge field has the magnitude

$$E_s = (kT/e)(1/n_e) \partial n_e / \partial r \quad (18)$$

and its radial average is of the order

$$\langle E_s \rangle \approx (kT/e)(1/R) \approx 13 \times 10^{-3} \text{ V/cm} \\ \text{for } T = 300 \text{ K.} \quad (19)$$

The estimate shows that the radial outflow of ions to the wall remains essentially unchanged by an electron-collecting probe. The argument against significant depletion of the plasma can be stated quite simply: Since the plasma seeks to remain electrically neutral, a depletion of electrons is possible only by removing ions, but the electric field produced by the probe is too small to remove the less mobile ions from the plasma. Hence there is no depletion.

A further, although minor point concerns the question of electron heating due to the small drift fields that will arise in the plasma. The effect can be estimated from known values of the characteristic energy (the D/μ ratio) for electrons drifting in helium at a field of 10^{-3} V/cm at a pressure of 1 Torr. The heating would be entirely negligible, even at fields ten times larger (see Fig. 14.1 in Ref. [10]).

Unfortunately, conditions can arise where the probe is unable to draw current at the expense of the wall current, and we encountered such effects in our experiments. It appears that sometimes the wall surfaces can be severely contaminated, in which case surface charges accumulate on nonconducting surface layers and the electron wall current becomes unusually small. The Langmuir probes

then cannot function properly since there is no wall current to be diverted to the probe. The effect can be drastic (see Sec. III B) and, unless one is aware of it, one may be misled into believing that the electron density is far lower than it actually is. We have not tested flow tubes made from nonconducting materials, for instance from glass, but it appears that rather large and well-cleaned reference electrodes would be needed to prevent depletion of the plasma. A problem may also arise when one attempts to use probes far upstream near the plasma inlet. Here, the probe current can easily approach the total current entering the tube and the probes then do not function as intended. In practice, this is not usually a problem since most flow tubes contain a fairly long section at the entrance to establish proper flow conditions.

III. EXPERIMENTAL MEASUREMENTS

The experiments were carried out with the goal of checking the internal consistency of the orbital-motion theory by testing several of its predictions, namely, (1) the square of probe current should depend linearly on the probe potential over a significant range, (2) in a quasineutral plasma containing only a single ion species of known mass, the ion current should be smaller by the square root of the electron-to-ion mass ratio, (3) the probe current should be linearly dependent on the probe surface area, and (4) the probe current should be proportional to the ion or electron density.

Ideally, an experiment should compare the measured electron and ion densities to results of an independent absolute measurement that employs a more rigorous method, such as microwave interferometry or microwave cavity frequency shift techniques. This has been done by others, although not in flowing-afterglow plasmas. There is, however, good indirect evidence in support of the absolute values of the measured electron densities from measurements of electron-ion recombination rate coefficients in flowing-afterglow plasma. Measurements of this type will be discussed later.

Two different sets of experiments were performed using two different flow tubes. In the first set of experiments, we investigated Langmuir probes of two different sizes in both the electron- and ion-collecting modes. The second set focused on a comparison of ion- and electron-density measurements, determinations of electron-ion recombination coefficients, and measurements of plasma velocities.

A. Measurements with two probes of different sizes

The flow tube used in the first set of experiments was a small and rather simple flowing-afterglow system employing a hollow-cathode discharge source, a stainless-steel flow tube (diameter of 3.65 cm), and a downstream mass spectrometer (see Fig. 2). The effective gas flow velocity was quite small, typically 1000 cm/s. Helium was admitted through the discharge at a pressure of 1.6 Torr and argon was added at a downstream gas inlet at a pressure of about 0.1 Torr to convert metastable helium atoms to argon ions. The only function of the mass spectrometer was to verify that Ar^+ ions were the dominant ion species in the plasma.

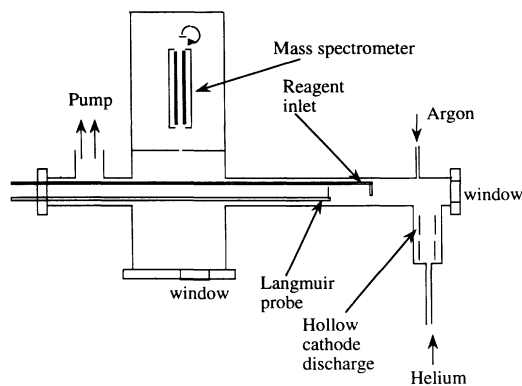


FIG. 2. Schematic diagram of the flow tube used in the measurements with two probes.

This simple apparatus had the advantage that the probes could be exchanged very quickly and that they could be observed visually through a glass window. Two cylindrical tungsten probes of different diameters (nominally 10 or 25 μm) and lengths (3.6 or 3.8 mm) were mounted parallel to each other on a movable support at a distance of about 4 mm from each other (see Fig. 3). The probes could be translated and rotated to the desired position while being viewed by a telescope. The probe wires were made from gold-plated tungsten, but the gold layer disappeared during the cleaning by electron bombardment. An effort was made to measure the diameters of the probe wires as precisely as possible. Direct measurements using mechanical micrometers were found to be too unreliable, especially for the smaller wire size. Better mechanical measurements were obtained by winding many turns of wire on a core and measuring the total length of many turns. Two optical methods were used; one employed optical diffraction of laser light from a helium-neon laser, the second consisted of projecting an enlarged image of the wires using a microscope lens. Samples of the thinner wire were also examined under a scanning electron microscope which showed that wires of this size are not perfectly uniform and have a consider-

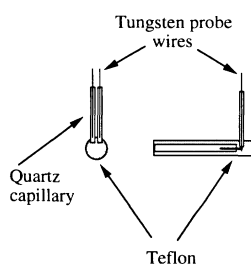


FIG. 3. Sketch of Langmuir probes used to compare probes of different sizes. The exposed part of the probe wire has a length of 4 to 5 mm. The spacing between wires is about 4 mm. The single probes used in the second set of experiments were constructed in the same way.

able surface roughness. Based on these measurements, we concluded that the smaller wire had a diameter of $10 \pm 1 \mu\text{m}$, and the larger wire a diameter of $25 \pm 3 \mu\text{m}$. By optical diffraction measurements, the ratio of the two wire diameters was found to be 2.44 ± 0.1 . Very fine quartz tubing was used to insulate part of the probe wire and to improve mechanical rigidity. The probe was oriented at a right angle with respect to the flow tube axis.

Initially, current-voltage probe curves were measured with a digital electrometer (Keithley Instruments Model 617) with a built-in precise voltage bias. Its analog output was recorded on a chart recorder. The electrometer had the advantage of precise voltage and current readings, but the bias voltages could be swept only slowly (about 1 to 10 s for a single sweep). A dependence of the probe curves on the rate and direction of the voltage sweep ("hysteresis" effect) was noticed only when operating the probe in the electron-collecting mode. Cleaning of the probe surface by drawing large electron currents from the plasma (up to 1 mA at 40 V, for several minutes) was found to be absolutely necessary to reduce hysteresis to tolerable levels. The residual hysteresis consisted mainly of small shifts along the voltage axis and had little effect on the slope of the I^2 vs V probe curves. As a rule, ion currents collected by the probes were far more stable and less sensitive to the prior history of a probe.

In later work, an electronic voltage-sweep circuit in conjunction with a differential amplifier followed by an analog squaring circuit was used and the probe curves were displayed on an x - y oscilloscope. The results were essentially the same as those obtained with the electrometer. This comment does not apply to the results obtained in the second flow tube (see Sec. III C), where significant differences were found between the results obtained with the electrometer and with the electronic sweep circuit.

B. Results of measurements with two different probe sizes

The probe curves obtained with the larger probe were generally very good in the sense that the square of the probe current varied linearly with the applied voltage up to quite large potentials of 8 V. This was true for both the ion and electron branches of the I - V characteristics.

In the case of the smaller probe, the I^2 vs V curves for the electron branch showed a significant upward curvature at large bias voltages. An example is shown in Fig. 4, where for ease of comparison the I^2 vs V curve for the smaller probe has been scaled up by the square of the ratio of probe surface areas. The initial slopes (below 1.5 V) of the curves are fairly close, but at higher voltages the discrepancy is quite evident. This suggests that only the initial slope of the I^2 vs V curves should be used to calculate the electron density. The smaller probe would have given larger electron densities (by about 45% in the example of Fig. 4) if the slope at higher voltages had been used in the analysis.

We tried to find a plausible explanation for the differing probe response at higher bias voltages, but no

clear conclusion was reached. It was thought that an upwards curvature of the I^2 vs V curves might be the "correct" behavior and that, in the case of the larger probe, the effect was compensated by either a depletion of electrons or a change in plasma potential. Experimental tests failed to support this conjecture. For instance, tests were made to detect changes of the plasma potential due to the presence of an electron-collecting probe. In one such test, the larger probe was biased positively (0 to 3 V) and the voltage of the smaller probe was measured with a high-impedance voltmeter. The test showed that the plasma potential relative to the chamber wall did not change by more than 10 mV. A further test was made in which the larger probe was biased positively (using fixed dc potentials from 0 to 10 V) and the current to the small probe was measured in the usual manner by sweeping the voltage. A fairly small (6%) reduction of the current collected by the small probe was observed when the larger probe was held at the large potential of 10 V. This observation indicates that the electron density in the probe vicinity can be depleted by an electron-collecting probe, but that the effect is fairly small.

The results obtained with the small electron-collecting probe show some disagreement with the orbital-motion theory, but if one limits the analysis to small voltages, the

problem can be circumvented. Probe measurements in the *ion-collecting* mode indicated a different and more serious problem. At the highest plasma densities (near 10^{10} cm^{-3} , as measured by electron-collecting probes) the smaller probe collected nearly the same ion current (about 80%) as did the larger probe even though its surface area was only 43% of that of the larger probe. Figure 5 shows an example of measured I^2 vs V curves. To bring out the discrepancy more clearly, the data for the small probe have been scaled up by the square of the surface ratio. At lower plasma densities (10^9 cm^{-3}) the currents collected by the two probes were essentially equal. This result is clearly inconsistent with the orbital-motion theory. If one were to use that theory to deduce densities, one would obtain different ion densities for probes of different size, neither of which would agree with the electron density obtained from the electron branch of the I - V curves. The larger probe would have given an ion density two to three times larger than the electron density, while the smaller probe would have given a four to six times higher density. We emphasize that the I^2 vs V curves were nevertheless quite linear, as was expected from the orbital-motion theory. Linearity of the I^2 vs V curves by itself clearly cannot be taken as evidence that the orbital-motion theory is applicable.

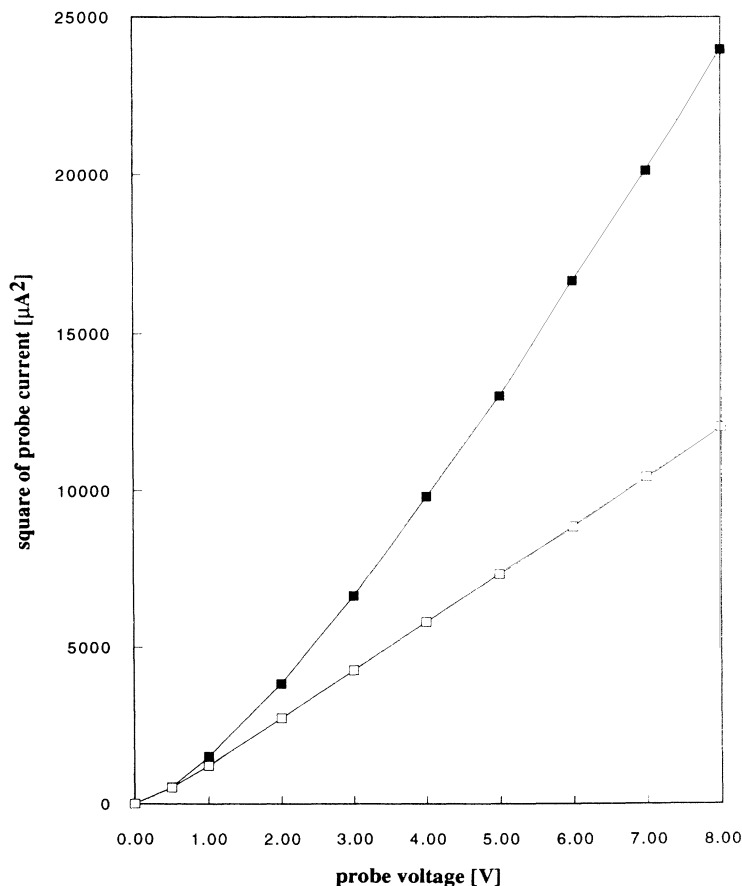


FIG. 4. I^2 vs V curves for electron-collecting probes of two sizes. Open squares: probe diameter, 25 μm ; probe length, 3.8 mm. Filled squares: probe diameter, 10 μm ; probe length, 3.6 mm. The currents of the small probe have been rescaled by the ratio of the probe surface areas. The electron density inferred from the larger probe is $4.3 \times 10^9 \text{ cm}^{-3}$.

C. Probe measurements of ion and electron densities in the fast flow tube

The first set of experiments gave us some insight into the behavior of probes in flowing-afterglow plasmas, but the conditions were not quite typical of most flow tube experiments. Most experiments use electrodeless microwave discharges as the plasma source and employ higher gas flow velocities. Therefore a second set of data were taken using a fast flow tube employing a microwave ionization source.

The basic features of the second flow tube were similar to those of the first, but the tube had a slightly larger diameter (4 cm) and it was equipped with a fast Roots pump that allowed operation at larger flow velocities (5000 cm/s). The plasma was generated in a microwave discharge in helium at pressures from 0.8 to 1.6 Torr, and, as before, argon was added to convert metastable helium ions to Ar^+ ions. A single Langmuir probe (diameter 27 μm , length 4 mm) was installed on a movable rod so that it could be positioned at any point on the axis of the flow tube.

The apparatus was equipped with calibrated flow meters and precise pressure gauges that allowed better flow characterization than was possible in the first apparatus. It was also possible, using the Langmuir probe, to ob-

serve the decay of the electron density as a result of electron-ion dissociative recombination when molecular gases were added to the plasma at a reagent inlet port. These measurements will be described here only to the extent that they provide a test of the probes.

As in the first set of experiments, the I^2 vs V curves for electrons and ions showed good linearity, but over a smaller range of bias voltages. Also, the rate at which the probe voltage was swept had a noticeable effect on the slope of the I^2 vs V curves. For instance, when the probe voltage was swept slowly (in 1 to 10 s) and the digital electrometer was used to measure the currents, the slopes of the I^2 vs V curves were consistently smaller by 10–20% than those obtained using the fast sweep circuit. As a rule, the I^2 vs V curves for ions were less sensitive to the voltage sweep rate than those for electrons. In order to find the “best” sweep rate, probe curves were recorded at various electron densities and sweep rates. The results showed that the I^2 vs V curves varied little with sweep rate in the range from 1 V in 0.1 s to 1 V in 10 μs . Most of the data were taken at sweep rates of 1 V in 5 ms.

It was also observed that the electron current began to “saturate” at smaller voltages when the probe was placed close to the plasma inlet. The cause of the saturation is most likely that the probe current then is limited by the

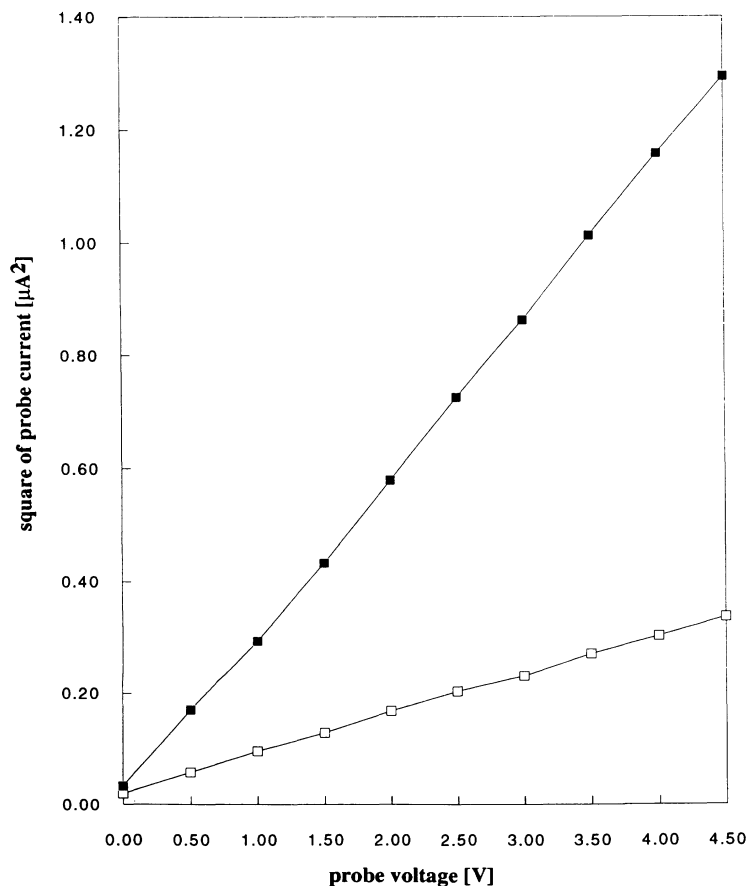


FIG. 5. I^2 vs V curves for ion-collecting probes of two sizes. The ions were Ar^+ . Open squares: probe diameter, 25 μm ; probe length, 3.8 mm. Filled squares: probe diameter, 10 μm ; probe length, 3.6 mm. The currents of the small probe have been rescaled by the ratio of the probe surface areas. The electron density was the same as in Fig. 4.

total electron current that enters the flow tube. At points further downstream, the linear range was larger, typically 2–3 V. Finally, at very low electron densities (below about 10^8 cm^{-3}), the I^2 vs V curves again became non-linear. The probe current I , rather than I^2 , varied linearly with voltage. This sets the lower limit of the range of electron densities that can be covered. Smith and Plumb [11] suggested that at very low densities the space charge sheath expands to such a size that the probe no longer has cylindrical symmetry.

In the course of this work, we twice observed a rather disturbing effect: The decline of the measured electron density as a function of position was perfectly normal in the upstream part of the tube, but it appeared to drop off rapidly once the electron density approached values of about $2 \times 10^9 \text{ cm}^{-3}$. By contrast, the ion densities measured with the probe exhibited the normal, slowly decaying behavior. This peculiar effect persisted for several weeks of operating the flow tube and then disappeared. The most likely explanation is that the surfaces of the (stainless-steel) tube were coated with an insulating layer that was eventually removed by the plasma.

One important result of these measurements is the comparison of the apparent electron and ion densities that were inferred from the data. Figure 6 shows the ratio of measured electron and ion densities, as calculated from the orbital-motion formula. The ions were almost entirely Ar^+ . The helium pressure was varied from 0.5 to 1.6 Torr and data were taken at different points in the flow tube to obtain the variation with electron density. The observed ratio n_i/n_e is seen to decrease by a factor of 2 at all electron densities as the pressure increases from 0.5 to 1.6 Torr. The result is clearly unacceptable since in a quasineutral plasma the true ratio should be close to unity at all pressures. Either the electron or the ion density or both must be given incorrectly by the orbital-

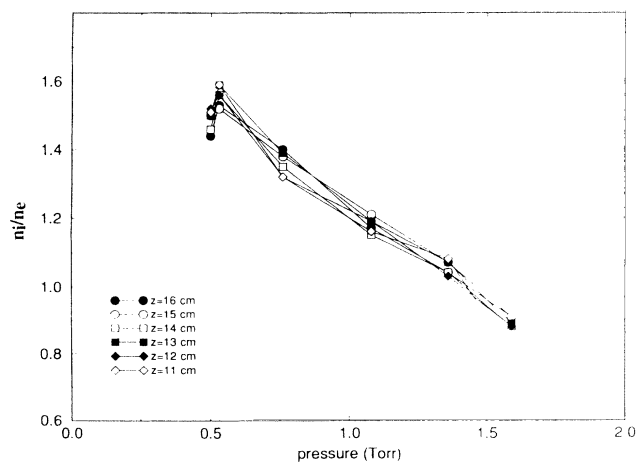


FIG. 6. Apparent ratios of the argon-ion and electron densities at different gas pressures and different positions in the fast flow tube. At $p = 1$ Torr, the electron density at position $z = 16$ cm was $n_e = 8 \times 10^9 \text{ cm}^{-3}$. At $z = 11$ cm it was $n_e = 3.95 \times 10^9 \text{ cm}^{-3}$.

motion theory, but it is not obvious which, if any, of the two densities can be trusted. The question was decided by remeasuring the known recombination coefficient of O_2^+ , which will be described in the next section.

D. Electron-ion recombination measurements

In these measurements, oxygen was added to convert by ion-molecule charge transfer the nonrecombining Ar^+ ions to O_2^+ ions that subsequently undergo dissociative recombination with electrons. The decay of the electron density as a function of position was analyzed to obtain the recombination coefficient of O_2^+ . Its value is known from the microwave afterglow studies of Mehr and Biondi [12] to be $(1.95 \pm 0.2) \times 10^{-7} \text{ cm}^3/\text{s}$ at an electron temperature of 300 K. Other measurements [13,14] support this recombination coefficient, but some of them also rely on Langmuir-probe measurements while others were normalized to the microwave afterglow value and are thus not truly independent.

In order to measure the recombination coefficient accurately, two computer models of the recombining plasma were constructed. In the first, the electron continuity equation

$$\begin{aligned} \partial n_e(z,r)/\partial z = & [1/v_{\text{gas}}(r)] \\ & \times \{ (D_a/r) \{ \partial/\partial r [r \partial n_e(z,r)/\partial r] \} \\ & - \alpha n_e(z,r)^2 \}, \end{aligned} \quad (20)$$

with $v_{\text{gas}}(r) = v_{\text{gas}}(r=0)[1 - (r/R)^2]$ is solved. Here, D_a is the ambipolar diffusion coefficient which can be deduced from zero-field mobility data, using Einstein's relation between diffusion and mobility. This treatment takes proper account of the radial dependence of n_e and the radial variation of the gas flow, but it ignores axial diffusion. The neglect of axial diffusion is not entirely justified since the axial gradients in a recombining plasma can easily approach the radial gradients. It should be incorporated into more accurate models.

In a second, simplified model the radial dependencies of n_e and v_{gas} , are ignored and diffusion losses are calculated assuming that a fundamental-diffusion-mode distribution is approximately valid in the recombining plasma. The electron continuity equation then can be written as

$$\partial n_e(r=0)/\partial z = - (1/v_{\text{eff}}) \{ n_e(r=0) \nu_d + \alpha n_e^2 \}, \quad (21)$$

where $\nu_d = D_a/\Lambda^2$ is the diffusion loss frequency and Λ is the fundamental diffusion length (for a cylinder, $\Lambda = R/2.405$). In this model, an effective flow velocity v_{eff} has to be used that is not equal to the average gas flow velocity $\langle v_{\text{gas}} \rangle = \frac{1}{2}v(r=0)$. A comparison of calculations made with the two models indicates that the simplified model is of adequate accuracy if one uses $v_{\text{eff}} = (1.7 \pm 0.1) \langle v_{\text{gas}} \rangle$. The exact factor depends on the relative magnitudes of the diffusion and recombination losses. The simplified model has the virtue that it is far easier to incorporate additional reactions (e.g., ion conversion) and was the preferred method of analysis.

From a large set of experimental data at different gas

pressures we obtained consistent values of the recombination coefficient $\alpha(\text{O}_2^+) = (2 \pm 0.2) \times 10^{-7} \text{ cm}^3/\text{s}$, in excellent agreement with the values obtained by the microwave afterglow method. Any possible error in the experimental determination of electron densities would have affected the inferred recombination coefficient so that the agreement must be regarded as strong support for the reliability of the electron-density measurements. This obviously implies that ion densities, for instance the argon-ion densities shown in Fig. 6, are not given correctly by the orbital-motion theory.

E. Measurements of plasma flow velocities

The analysis of the recombining plasma depends critically on the effective flow velocity v_{eff} . It is common practice to use Langmuir probes to determine the flow velocity of the plasma by modulating the plasma source and monitoring the passage of the maximum electron density at two or more locations in the flow tube. While this measurement is quite simple to perform, its interpretation deserves some scrutiny. In an early application of the technique, Adams, Church, and Smith [15] compared the velocity obtained in this manner to an average "plasma velocity" that was defined as

$$\langle v_p \rangle = (1/\langle n_e \rangle) \int_0^R n_e(z_p, r) v_{\text{flow}}(r) 2\pi r dr, \quad (22)$$

where

$$\langle n_e \rangle = \int_0^R n_e(z_p, r) 2\pi r dr.$$

Adams, Church, and Smith show that $\langle v_p \rangle \approx \frac{4}{3} \langle v_{\text{flow}} \rangle$ for a fundamental-mode radial electron density distribution. The numerical solution of the electron continuity equation yielded $\langle v_p \rangle \approx 1.41 \langle v_{\text{flow}} \rangle$, quite close to the approximate value $\frac{4}{3}$. Our attempts to verify the factors $\frac{4}{3}$ or 1.41 experimentally by comparing the average gas flow velocity (obtained from calibrated gas flow meters and pressure gauges) to the measured pulse propagation velocity were quite unsuccessful. Typically, we obtained numbers of 1.8 rather than $\frac{4}{3}$. It became clear eventually that the so-called average plasma velocity differs considerably from the propagation velocity of a plasma pulse or the velocity of the modulation envelope. Two different physical concepts are involved: $\langle v_p \rangle$ is the average flow velocity of electrons through a cross section of the tube while the propagation velocity of a pulse is inferred from the delay time between arrival at two different locations, i.e.,

$$\langle v_{\text{prop}} \rangle = (z_2 - z_1)/(t_2 - t_1). \quad (23)$$

The pulse arriving at the second location, however, has a different time dependence and it consists only of those electrons that have not diffused very far from the flow tube axis. Since the gas flow velocity has the highest value on axis, a pulse will propagate with a velocity that is higher than the average defined by Eq. (22). It was found difficult to solve the problem analytically, but some insight was gained by a simple random-walk computer simulation. In the simulation, a test particle was made to

execute a three-dimensional random walk in a simulated parabolic flow. Particles were eliminated whenever they diffused outside the tube radius. The computer recorded the times when the test particles passed through two "gates" located at positions z_1 and z_2 , displayed the distribution of arrival times, and calculated the velocities. The gates simulate the Langmuir probes that are used in the experiment. The location of the first gate was chosen so that the test particle had a $1/e$ probability of surviving to the first gate. Even after several thousand iterations, the results suffered somewhat from poor statistics, but it was nevertheless clear that velocities were close to 1.8 times larger than the average gas flow velocities, in agreement with the experimental findings. The results of the simulation depended slightly on the size of the gate (circular disks of $\frac{1}{16}$ to $\frac{1}{4}$ of the tube cross section, centered on the axis).

The computer simulation and the experimental results show that average plasma velocity, as defined by Eq. (22), is not identical to the propagation velocity. If we had used the average plasma velocity in our analysis of the recombining plasma, we would have obtained $\alpha(\text{O}_2^+) = 1.5 \times 10^{-7} \text{ cm}^3/\text{s}$. Fortunately, only a small error results if one uses the *measured* propagation velocity ($1.8 \langle v_{\text{gas}} \rangle$) instead of the effective velocity ($1.7 \langle v_{\text{gas}} \rangle$) in the analysis of recombination data by Eq. (21), as is common practice.

IV. SUMMARY AND CONCLUSIONS

Our results support the orbital-motion analysis of Langmuir probes only if they are used in the electron-collecting mode. The densities deduced from electron-collecting probes of different sizes are consistent provided that the probe currents at low voltages are used in the analysis. Recombination measurements confirm that the absolute values are quite accurate (about 10%). These findings corroborate the work by other experimentalists.

Serious perturbations of the plasma by the probes were observed only when the reference electrodes were contaminated, but otherwise they seem to be surprisingly small. Probes of small radius show greater deviations from the orbital-motion theory and do not seem to offer a significant advantage compared to the commonly used size of 25 μm .

Our results also show, however, that the orbital-motion theory fails for ion-collecting probes. The experiments show that the probe currents do not scale correctly with the probe surface area and that the inferred ion densities are not in agreement with measured electron densities. It also appears that the response of ion-collecting probes depends on gas density. This is not the first result that casts doubt on the validity of the orbital-motion theory for ion-collecting probes. Similar, but smaller effects have been noted in stationary afterglow plasmas [16] and more drastic discrepancies between ion and electron densities have been found in discharge plasmas [3]. Strong negative dependencies of the probe current on gas density have also been observed [7]. On the other hand, some investigators [2] have used ion-collecting probes to obtain data on the pressure dependence of ion-ion recombina-

tion rate coefficients (at pressures up to 8 Torr), implying that such probes might be well suited for flowing-afterglow studies. We must conclude that this is not the case and now regard the results on ion-ion recombination rates and the inferred variation of the recombination coefficients with gas density with some caution.

The use of Langmuir probes to measure flow velocities is found to be useful and quite accurate, but one should be aware that the measured velocities are not the same as the so-called average plasma velocity.

The question remains of why the orbital-motion theory fails for ion-collecting probes. It appears likely that the energy-reducing collisions between ions and atoms lead to trapping of ions in the potential well surrounding the

probe. A trapped ion will suffer further energy-reducing collisions and eventually strike the probe. The target area of the probe then largely depends on the density of atoms and the ion-atom collision cross section, rather than on the surface area of the probe. Our measurements using two different probe sizes support this picture. It is possible that the orbital-motion theory may give better results for probes that are even larger than those used here and this may be worth exploring.

ACKNOWLEDGMENT

This work was supported, in part, by NASA under Grant No. NAGW-1764.

-
- [1] D. Smith, N. G. Adams, A. G. Dean, and M. J. Church, *J. Phys. D* **8**, 141 (1975).
- [2] D. Smith and N. G. Adams, in *Physics of Ion-Ion and Electron-Ion Collisions*, edited by F. Brouillard and J. Wm. McGowan (Plenum, New York, 1982), p. 501.
- [3] I. C. Sudit and P. C. Woods (unpublished); I. C. Sudit, Ph.D. thesis, University of Wisconsin, Madison, 1992, and private communication.
- [4] P. M. Chung, L. Talbot, and K. J. Touryan, *AIAA J.* **12**, 133 (1974).
- [5] H. M. Mott-Smith and I. Langmuir, *Phys. Rev.* **28**, 727 (1926).
- [6] R. T. Bettinger and E. H. Walker, *Phys. Fluids* **8**, 748 (1965).
- [7] G. J. Schulz and S. C. Brown, *Phys. Rev.* **98**, 1642 (1955).
- [8] For a recent review see M. R. Flannery in *Advances in Atomic, Molecular, and Optical Physics*, edited by B. Bederson and A. Dalgarno (Academic, New York, 1994), Vol. 32, p. 117.
- [9] M. Hayashi and S. Ushiroda, *J. Chem. Phys.* **78**, 2621 (1983).
- [10] L. G. H. Huxley and R. W. Crompton, *The Diffusion and Drift of Electrons in Gases* (Wiley, New York, 1974).
- [11] D. Smith and I. C. Plumb, *J. Phys. D* **5**, 1226 (1972).
- [12] F. J. Mehr and M. A. Biondi, *Phys. Rev.* **181**, 264 (1996).
- [13] E. Alge, N. G. Adams, and D. Smith, *J. Phys. B* **16**, 1433 (1983).
- [14] R. Johnsen, *Int. J. Mass Spectrom. Ion Proc.* **81**, 67 (1987).
- [15] N. G. Adams, M. J. Church, and D. Smith, *J. Phys. D* **8**, 1409 (1975).
- [16] D. Smith and I. C. Plumb, *J. Phys. D* **6**, 196 (1973).

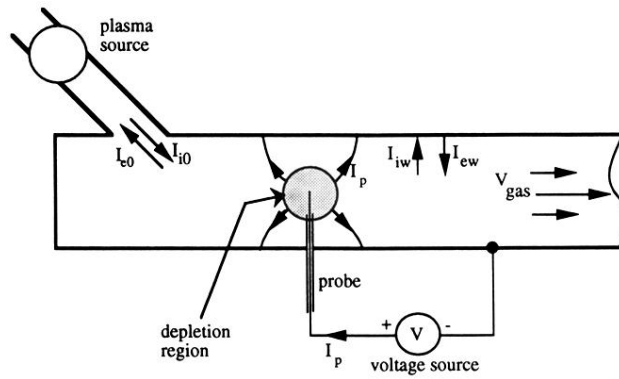


FIG. 1. Schematic diagram of electron and ion currents entering the flow tube from the discharge and leaving to either the probe or the flow tube wall.

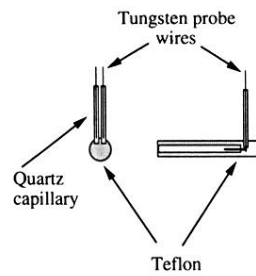


FIG. 3. Sketch of Langmuir probes used to compare probes of different sizes. The exposed part of the probe wire has a length of 4 to 5 mm. The spacing between wires is about 4 mm. The single probes used in the second set of experiments were constructed in the same way.